

A hybrid model of regional path loss of wireless signals through the wall

Guangyong Xi^{1*}, Shizhen Lin², and Dongyao Zou¹

¹ College of Computer and Communication Engineering, Zhengzhou University of Light Industry
Zhengzhou, Henan 450000 China
[e-mail: xigy@zzuli.edu.cn, zdy@zzuli.edu.cn]

² Shandong Eastdawn Corporation
Jinan, Shandong 250101 China
[e-mail: linhengqian@163.com]

*Corresponding author: Guangyong Xi

*Received May 22, 2022; revised August 4, 2022; accepted September 6, 2022;
published September 30, 2022*

Abstract

Wall obstruction is the main factor leading to the non-line of sight (NLoS) error of indoor localization based on received signal strength indicator (RSSI). Modeling and correcting the path loss of the signals through the wall will improve the accuracy of RSSI localization. Based on electromagnetic wave propagation theory, the reflection and transmission process of wireless signals propagation through the wall is analyzed. The path loss of signals through wall is deduced based on power loss and RSSI definition, and the theoretical model of path loss of signals through wall is proposed. In view of electromagnetic characteristic parameters of the theoretical model usually cannot be accurately obtained, the statistical model of NLoS error caused by the signals through the wall is presented based on the log-distance path loss model to solve the parameters. Combining the statistical model and theoretical model, a hybrid model of path loss of signals through wall is proposed. Based on the empirical values of electromagnetic characteristic parameters of the concrete wall, the effect of each electromagnetic characteristic parameters on path loss is analyzed, and the theoretical model of regional path loss of signals through the wall is established. The statistical model and hybrid model of regional path loss of signals through wall are established by RSSI observation experiments, respectively. The hybrid model can solve the problem of path loss when the material of wall is unknown. The results show that the hybrid model can better express the actual trend of the regional path loss and maintain the pass loss continuity of adjacent areas. The validity of the hybrid model is verified by inverse computation of the RSSI of the extended region, and the calculated RSSI is basically consistent with the measured RSSI. The hybrid model can be used to forecast regional path loss of signals through the wall.

Keywords: RSSI, signals propagation through the wall, NLoS, path loss

The research has been funded by Key scientific and technological projects in Henan Province, grant number 212102210407 and 192102210133.

1. Introduction

Due to the advantages of lower computational requirements and readily available hardware, wireless local area networking (WLAN) has been widely used in military surveillance, industrial process control and environmental monitoring [1-3]. Recently, indoor localization based on WLAN has attracted significant research attention and growing interest [4]. The indoor localization algorithms can be divided into two categories: range-based and range-free. Typical range-based localization algorithms include time of arrival (TOA), time difference of arrival (TDOA), angle of arrival (AOA) and received signal strength indicator (RSSI), which have higher accuracy than that of range-free [3]. RSSI is widely used in indoor localization because its low power consumption and no additional hardware required. However, there are various obstacles in the actual indoor environment, such as wall, door and furniture, which will cause the NLoS interference in the wireless signals propagation path [5]. Wireless signals through the obstacle environment are affected by diffraction, reflection and scattering, which will cause RSSI attenuation and fluctuation [6-7]. Among the observation errors of RSSI, the NLoS caused by signals reflection and transmission path loss when wireless signals through the wall, is the main factor affecting the indoor localization accuracy. The ranging error caused by NLoS can reach 20%-50% of the communication radius [8]. Therefore, the key to wireless indoor localization using RSSI is to analyze the path loss of signals through the wall and establish the mathematical models.

At present, the research on the path loss of wireless signals through the medium focuses on the theoretical method and the empirical method. The theoretical method usually adopts deterministic or semi-deterministic methods to study the signal attenuation characteristics based on the propagation theory and physical laws of electromagnetic wave and numerical simulation. The finite element method (FEM), the plane wave expansion (PWE) method and the finite difference time domain (FDTD) method are used to simulate and analyze the propagation characteristics of electromagnetic wave through the medium [9-14]. According to the influence of the permittivity, conductivity, permeability, incident frequency and incident angle on reflection coefficient and transmission coefficient, the attenuation characteristics of wireless signals through the medium are obtained. However, each of these methods has its drawbacks, such as high complexity, large amount of calculation [9]. In addition, it's difficult to accurately obtain the actual permittivity, conductivity and permeability of medium.

The empirical method composes of deterministic method and statistical method. Statistical method is based on the empirical path loss models of wireless signals propagation and RSSI observations. The popular empirical path loss models, such as Okumura-Hata, COST 231, Keenan-Motley model and log-distance path loss model are the most widely used for path loss predictions [15-16]. The advantages of empirical path loss models are easier to implement than theoretical path loss models [6]. Moreover, stepwise regression, genetic algorithm, particle swarm optimization and machine learning are used to establish the empirical path loss model [6,17-18]. However, due to the observations error of RSSI, the calculated path loss has the irregular fluctuations and discontinuity of adjacent areas.

In order to obtain the actual regional path loss of wireless signals through wall, we propose a hybrid path loss model by combining theoretical and empirical models. The propagation process of wireless signals through the wall is divided into three sections, and the power loss relation between each key point is deduced based on incident angle, thickness and electromagnetic characteristic parameters of the wall. According to the power loss and RSSI definition, the path loss of signals through the wall is deduced, and the theoretical model of signals through the wall is established. Combined with the theoretical and empirical models

of path loss, the electromagnetic characteristic parameters in the hybrid model are solved. The hybrid model of path loss can improve the path loss accuracy and maintain the spatial continuity of regional path loss.

The rest of this paper is organized as follows. In Section 2, we analyze the path loss process of wireless signals propagation through the wall, describe the establishment of theoretical model and empirical model of path loss, and present the hybrid model of path loss. In section 3 we describe our experiments and analyze the effect of each electromagnetic characteristic parameters on path loss, and the validity of the hybrid model for regional path loss is discussed. Finally, some conclusions from this study are given in section 4.

2. Modeling of path loss of wireless signals through the wall

2.1 The path loss process of wireless signals propagation through the wall

The propagation process of wireless signals through the wall can be divided into three sections: before the incidence of the wall, through the wall and after output of the wall. During the propagation of signals through the wall, reflection and transmission of signals occur. From the transmitting node Tn to the receiving node Rn , the propagation paths are TnA , $A'B'$ and BRn , respectively. The directions of reflection and transmission of signals incident-point A are AA'' and AA' , respectively. The directions of reflection and transmission of signal output-point B' are $B'B''$ and $B'B$, respectively. The propagation process of wireless signals through the wall is shown in Fig. 1.

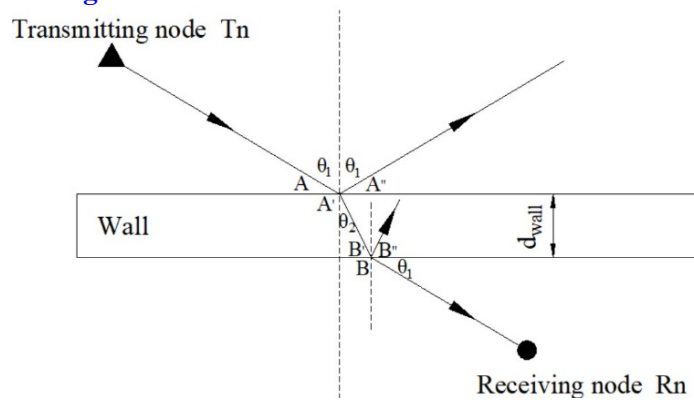


Fig. 1. The propagation process of wireless signals through the wall

P_{Tn} is set as the power of transmitting node Tn , P_{Rn} is the power of receiving node Rn . P_A , $P_{A'}$, $P_{B'}$ and P_B are the power of incident-point A , point A' , point B' and output-point B , respectively. The power unit is mw , and the power relationship at A , point A' , point B' and output-point B is [19]:

$$\begin{cases} P_{A'} = (1-R_A)P_A \\ P_{B'} = P_{A'}e^{-2\alpha l} \\ P_B = (1-R_B)P_{B'} \end{cases}, \tag{1}$$

where R_A and R_B are the power reflection coefficient of point A and point B , respectively. α is the attenuation constant of signals through the wall, and l is the propagation distance of signals in the wall.

The power reflection coefficients R_A and R_B are functions of signal reflection coefficient τ_A and τ_B , respectively. R_A and R_B are calculated in the same way. Take R_A as an example, and can be expressed as [20-21]:

$$R_A = |\tau_A|^2 = \frac{\left| \cos \theta_1 - \sqrt{\frac{\varepsilon_2}{\varepsilon_1} - \sin^2 \theta_1} \right|^2}{\left| \cos \theta_1 + \sqrt{\frac{\varepsilon_2}{\varepsilon_1} - \sin^2 \theta_1} \right|^2}, \quad (2)$$

where ε_1 and ε_2 are the permittivity of air and wall, respectively. θ_1 is the incident angle, θ_2 is the transmission angle in the wall. Based on Snell's law of refraction, the incident angle and transmission angle have the following relation [22]:

$$\frac{\sin \theta_2}{\sin \theta_1} = \sqrt{\frac{\varepsilon_1}{\varepsilon_2}} = \sqrt{\varepsilon_r}, \quad (3)$$

where the ratio of ε_1 to ε_2 is defined as the relative permittivity ε_r .

Since air and wall are weak loss media, the attenuation constant of signal through the wall can be approximately expressed as [19]:

$$\alpha = \omega \sqrt{\varepsilon_2 \mu_2} \sqrt{\frac{1}{2} \left[\sqrt{1 + \frac{\sigma_2^2}{\omega^2 \varepsilon_2^2}} \right]} \approx \frac{1}{2} \sigma_2 \sqrt{\frac{\mu_2}{\varepsilon_2}}, \quad (4)$$

where ω is angular frequency, σ_2 , μ_2 are the conductivity and permeability of the wall, respectively.

Combined with equation (3), the propagation distance l of signals in the wall can be expressed as:

$$l = \frac{d_{\text{wall}}}{\cos \theta_2} = \frac{d_{\text{wall}}}{\sqrt{1 - \frac{\varepsilon_1}{\varepsilon_2} \sin^2 \theta_1}}, \quad (5)$$

where d_{wall} is the thickness of wall.

2.2 Theoretical model of path loss of signals through the wall

The path loss of wireless signals caused by the wall, including reflection and transmission loss, can be calculated by the total loss of the transmitting node to the receiving node minus the path loss of TnA and BRn . According to the definition of path loss, the total loss from transmitting node Tn to receiving node Rn is [23-24]:

$$PL_{\text{total}[dB]} = P_{Tn[dBm]} - RSSI_{Rn[dBm]} \quad (6)$$

Similarly, the path loss from transmitting node Tn to point A is:

$$PL_{TnA[dB]} = P_{Tn[dBm]} - RSSI_{A[dBm]} \quad (7)$$

Combined with equation (1), the path loss from point B to receiving node r is:

$$PL_{BRn} = \frac{P_{B[mw]}}{P_{Rn[mw]}} = \frac{(1-R_B)(1-R_A)e^{-2\alpha l} P_{A[mw]}}{P_{Rn[mw]}} \quad (8)$$

The unit of path loss converted into dBm can be expressed:

$$PL_{BRn[dB]} = 10 \lg(1-R_B)(1-R_A)e^{-2\alpha l} + RSSI_{A[dBm]} - RSSI_{Rn[dBm]} \quad (9)$$

Therefore, the loss caused by wall reflection and transmission is:

$$PL_{wall[dB]} = PL_{total[dB]} - PL_{TnA[dB]} - PL_{BRn[dB]} = -10\lg(1-R_B)(1-R_A)e^{-2\alpha l} \quad (10)$$

If the incident angle, permittivity, conductivity and permeability of the wall can be accurately obtained, the theoretical model of path loss of signals through the wall can be established. The advantage of the theoretical model of path loss of wireless signals through the wall is that it can reflect the law of signals attenuation by wall and maintain the regional continuity of path loss. However, the permittivity, conductivity and permeability of wall usually cannot be accurately obtained, which limits the practical application of the theoretical model.

2.3 Statistical model of path loss of signals through the wall

Statistical model can be established by the empirical path loss models of wireless signals propagation and RSSI observations. The most commonly used empirical model is log-distance path loss model because of its accuracy and convenience [25]. The statistical model of the path loss of signals through wall is based on the total loss from the transmitting node to the receiving node, minus the path loss of the same distance of line of sight (LoS), which is calculated by statistical method. When there is no wall barrier between the transmitting node and the receiving node, the LoS path loss can be expressed as [5, 25]:

$$PL_{LoS[dB]} = P_{Tn[dBm]} - RSSI_{d_0[dBm]} + 10\eta \lg\left(\frac{d_{TnRn}}{d_0}\right) \quad (11)$$

where, d_0 is the reference distance, $RSSI_{d_0}$ is the signal strength with distance of d_0 from transmitting node, d_{TnRn} is the distance between transmitting node and receiving node. η is the regional path loss index, which can be calculated by statistics of the transmitting node and multiple receiving nodes before the incidence of the wall.

Combined with equation (6), the NLoS error caused by wall is:

$$PL_{NLoS[dB]} = PL_{total[dB]} - PL_{LoS[dB]} = RSSI_{d_0[dBm]} - RSSI_{Rn[dBm]} - 10\eta \lg\left(\frac{d_{TnRn}}{d_0}\right) \quad (12)$$

The statistical model of path loss caused by wall can be established by RSSI at d_0 from the transmitting node, RSSI at the receiving node, and regional path loss index. The statistical model of signals path loss through the wall is based on the RSSI observations, which can better reflect the actual environment of signals attenuation. However, since η solved by the least square method reflects the path loss index of the region, and RSSI has observation error, the established path loss statistical model has large error at some observation points. The calculated path loss by the statistical model has the irregular fluctuations and discontinuity of adjacent areas.

2.4 Hybrid model of path loss of signals through the wall

In practice, the path loss of the theoretical model PL_{wall} and the path loss of the statistical model PL_{NLoS} should be approximately equal. Therefore, combining the theoretical model established by equation (10) and the statistical model established by equation (12), a hybrid model can be established as:

$$RSSI_{d_0[dBm]} - RSSI_{Rn[dBm]} - 10\eta \lg\left(\frac{d_{TnRn}}{d_0}\right) = -10\lg(1-R_B)(1-R_A)e^{-2\alpha l} \quad (13)$$

Based on RSSI observations and calculated regional path loss index η , the least square method is used to solve the relative permittivity ϵ_r and the attenuation constant α of the wall.

The solved ε_r and α can be substituted into equation (10) to solve the path loss of wireless signals through the wall. Then, the regional path loss of wireless signals through wall can be solved.

The Hybrid model is based on theoretical model and statistical model, and its modeling process includes both models, with the main steps of this modeling process described in [Algorithm 1](#).

Algorithm 1 The Hybrid modeling process

Input: Transmitting power P_{Tn} , distance between Tn1 and Tn2, $RSSI_{d_0}$ of reference distance d_0 , incident angle θ_1 , RSSI observations

Step 1: Calculate the regional path loss index η under line-of-sight condition, using RSSI observations of each receiving node in front of the wall and logarithmic distance path loss model;

Step 2: Calculate the NLoS error PL_{NLoS} under non-line of sight condition based on RSSI observations of each receiving node behind the wall, the regional path loss index η and logarithmic distance path loss model;

Step 3: Combine the theoretical model and the statistical model, calculate the relative permittivity ε_r and the attenuation constant α , using RSSI observations of each receiving node behind the wall and the least square method;

Step 4: Substitute the relative permittivity ε_r and the attenuation constant α into the theoretical model;

Output: The regional path loss of signals through the wall

3. Experimental Results and Analysis

This section consists of four main parts: the RSSI observation experiment of wireless signals through the wall, the theoretical model established by the empirical values of electromagnetic characteristic parameters of the concrete wall, the hybrid model of path loss through wall established based on RSSI observations, and the validity of the hybrid model for regional path loss.

3.1 The RSSI observation experiment of wireless signals through the wall

In order to analyze the path loss of signals through the wall, the RSSI observation experiment is designed. The experiment is carried out on the second floor of the gymnasium. The internal dimensions of the lounge are 8m long and 4.8m wide, and the outside of the lounge is a capped terrace. The thickness of the concrete wall is 0.24m, and the wall material is unknown. The transmitting node is placed in the lounge, and located at Tn1 (-1, 0) and Tn2 (-2, 0) in turn. The receiving node is deployed on each grid point of the lounge and terrace, and the grid spacing is 0.5 m. The definition of the coordinate system, nodes distribution and region division of the RSSI observation experiment are shown in [Fig. 2](#). The transmitting node and receiving node are ZigBee module (2.4G), and fixed on the tripod with height of 1.5m. The transmitting node is powered by USB mobile power supply. The laptop is connected to the receiving node, supplies power to the receiving node and stores data. The transmitting power is 4.5dBm, the sampling interval is 0.1s, and the sampling time of each grid point is 10min. The scene and measurement of the RSSI observation experiment of signals through the wall

are shown in Fig. 3.

The receiving nodes are distributed in three zones. The RSSI observations of each receiving node in zone *I* are used to calculate the path loss index of the region. The RSSI observations of each receiving node in zone *II* are used to establish the statistical model and the hybrid model of path loss of signals through the wall. The RSSI observations of each receiving node in zone *III* are used to verify the effect of the established model.

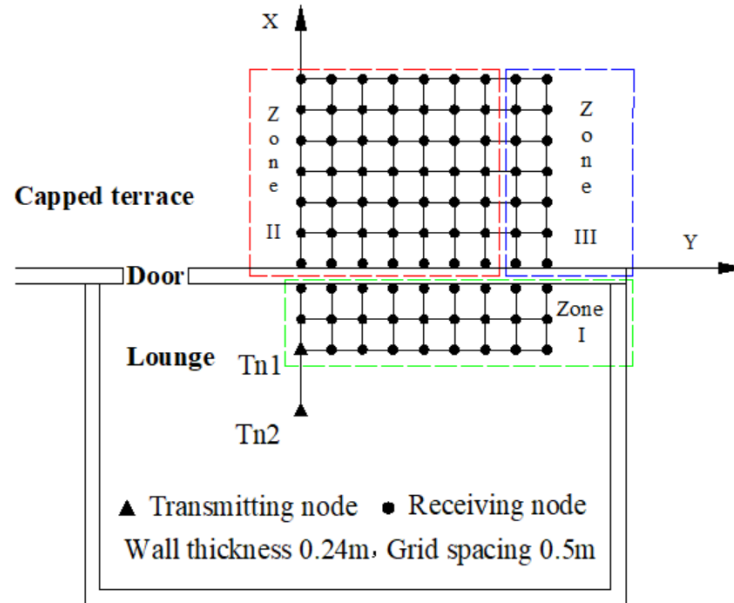


Fig. 2. The definition of the coordinate system, nodes distribution and region division of the RSSI observation experiment



Fig. 3. The scene and measurement of the RSSI observation experiment

3.2 The theoretical model established by the empirical values of electromagnetic characteristic parameters of the concrete wall

3.2.1 The effect of electromagnetic characteristic parameters on path loss

Given the relative permittivity, attenuation constant and wall thickness, the theoretical model of path loss of signals through the wall can be established based on the equation (10). Therefore, empirical values for these parameters can be used if the wall material is known. Researchers

have studied the electromagnetic properties of concrete walls [26-28]. In the literature [26], Kaplanvural et al tested the relative permittivity according to the water content of concrete, and the value range of relative permittivity was 0.1764 to 0.4202, with an average value of 0.247. In the literature [27], Ramaniraka et al showed that the absorption attenuation constants of concrete are 7 and 9 Np/m, with an average value of 8. In the literature [28], Stone carried out the experiments of electromagnetic signal attenuation in concrete walls with thickness of 0.102m, 0.203m and 0.305m, respectively. Since the wall thickness measured in the experiment is 0.24m, the effect of 0.24m wall thickness on path loss is simulated simultaneously. According to the parameters of concrete wall mentioned above, the path loss of theoretical model of signals through the wall can be simulated, and the relationship between path loss and relative permittivity, attenuation constant and wall thickness can be analyzed. The values of relative permittivity, attenuation constant, wall thickness and incident angle are shown in **Table 1**.

Table 1. The values of relative permittivity, attenuation constant, wall thickness and incident angle.

| relative permittivity ϵ_r | attenuation constant α (Np/m) | wall thickness d_{wall} (m) | incident angle ($^\circ$) |
|------------------------------------|--------------------------------------|-------------------------------|-----------------------------|
| [0.1764, 0.247, 0.4202] | [7, 8, 9] | [0.102, 0.203, 0.24, 0.305] | [0, 1, 2, ..., 89] |

In order to analyze the effect of each parameter on the path loss at different incident angles, one parameter is varied while the other parameters take intermediate values. When $d_{wall}=0.24$ and $\alpha=8$, the path loss at different relative permittivity varies with incident angle as shown in **Fig. 4**. When $d_{wall}=0.24$ and $\epsilon_r=0.247$, the path loss at different attenuation constant varies with incident angle as shown in **Fig. 5**. When $\alpha=8$ and $\epsilon_r=0.247$, the path loss at different wall thickness varies with incident angle as shown in **Fig. 6**.

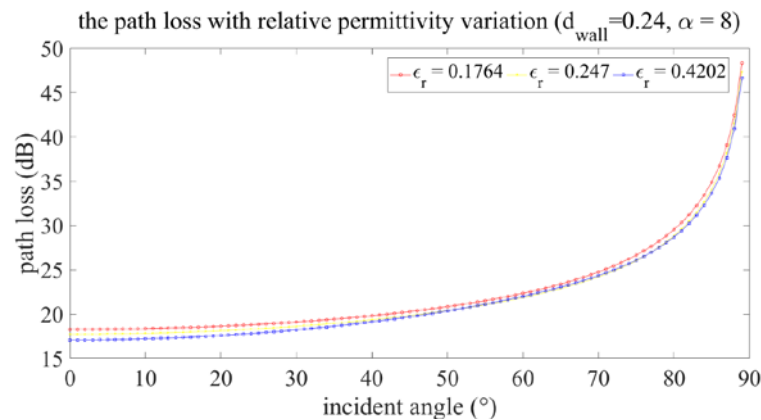


Fig. 4. The path loss at different relative permittivity varies with incident angle

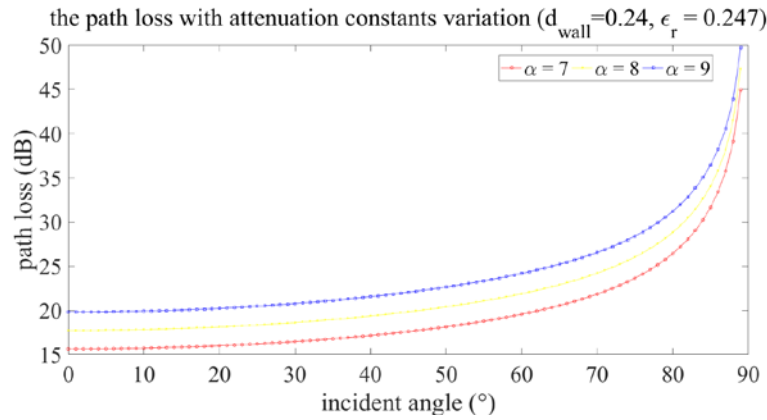


Fig. 5. The path loss at different attenuation constant varies with incident angle

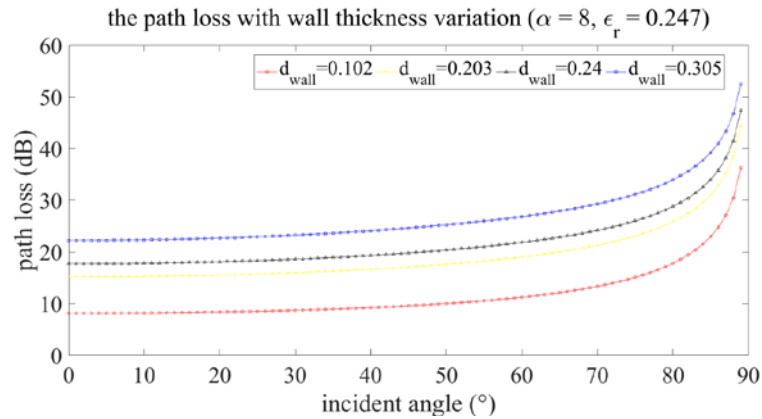


Fig. 6. The path loss at different wall thickness varies with incident angle

It can be seen from Fig. 4, Fig. 5 and Fig. 6 that the path loss increases with the increase of incident angle. The path loss increases slowly with the incident angle from 0° to 70° , and the path loss increases sharply with the incident angle from 70° to 89° . The wall thickness has a great influence on the path loss, followed by the attenuation constant, and the relative permittivity has a small influence on the path loss.

3.2.2 Regional path loss based on theoretical model and empirical values of electromagnetic characteristic parameters

Based on the empirical values of electromagnetic characteristic parameters of concrete wall and equation (10), the theoretical model of signal path loss through the wall can be established. Since the coordinates of each grid points are known, the angle between the line of transmitting node and receiving node and the wall can be solved. The range of angle between the line of Tn1(-1,0) and receiving nodes is 0° to 67.7064° , and the range of angle between the line of Tn1(-2,0) and receiving nodes is 0° to 53.3753° . The maximum value of the above two angle ranges is less than 70° . The angle between the line of transmitting node and receiving node and the wall has little effect on the path loss, and the angle can be approximated as the incident angle. The path loss of zone II corresponding to Tn1(-1,0) and Tn2(-2,0) are shown in Fig. 7 and Fig. 8, respectively.

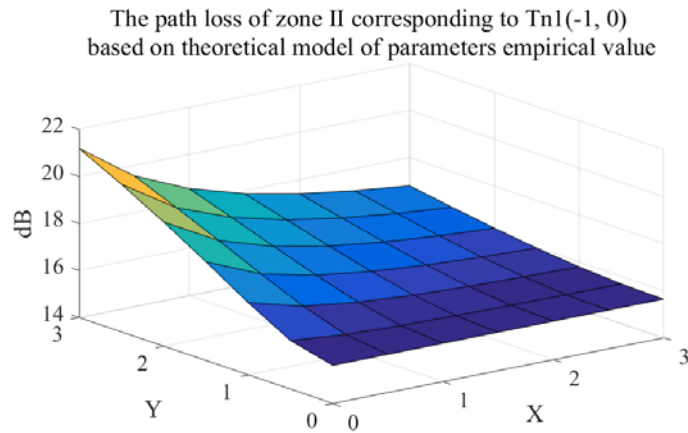


Fig. 7. The path loss of zone II corresponding to Tn1(-1,0) based on theoretical model of electromagnetic characteristic parameters empirical value ($\epsilon_r=0.247$, $\alpha=8$, $d_{wall}=0.24$)

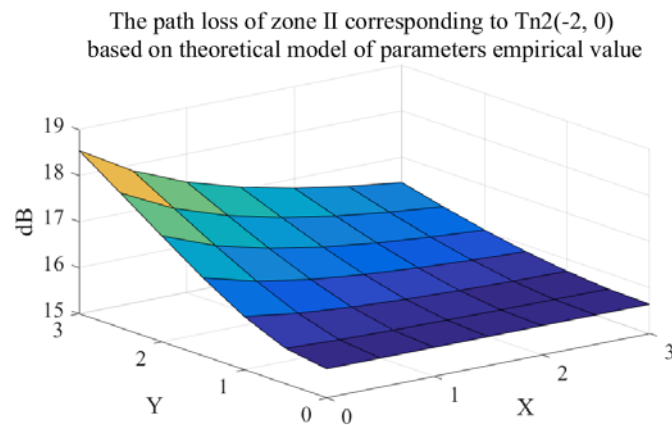


Fig. 8. The path loss of zone II corresponding to Tn2(-2,0) based on theoretical model of electromagnetic characteristic parameters empirical value ($\epsilon_r=0.247$, $\alpha=8$, $d_{wall}=0.24$)

It can be seen from **Fig. 7** and **Fig. 8** that the path loss solved by the theoretical model changes with the position relationship between different transmitting node and receiving node. The path loss increases with the increase of incident angle, and maintains the continuity in adjacent areas. With the increase of incident angle, the signals reflection increases and the transmission decreases, which leads to the increase of the path loss with the increase of the incident angle. However, due to the empirical value of the electromagnetic characteristic parameters of the concrete wall are used, the calculated path loss of the wall is usually inconsistent with actual path loss. Furthermore, if the wall material is unknown, the electromagnetic characteristics of the wall cannot be obtained, and the theoretical model of the path loss of the wireless signals through the wall cannot be established.

3.3 The hybrid model of path loss of signals through the wall established based on RSSI observations

Based on the power of transmitting nodes Tn1(-1,0), Tn2(-2,0) and the RSSI observations of each receiving node, the RSSI observations are denoised by Kalman filter. The fluctuation range of RSSI is 2-5dbm, and the mean value is taken to participate in modeling. Using the

RSSI of each receiving node in zone *I* and formula (11), the calculated regional path loss index of LoS is $\eta=1.7787$. Using the denoising RSSI of each receiving node in zone *II*, the statistical model and the hybrid model of the path loss through the wall can be established by equation (12) and equation (13), respectively. The relative permittivity ϵ_r and the attenuation constant α of the wall are solved. Introduce the solved ϵ_r and α into formula (10), then the path loss through the wall is obtained. The model parameters are shown in **Table 2**, and the RMSE is the root mean square error of the hybrid model. The path loss of zone *II* based on the statistical model and RSSI observations is shown in **Fig. 9** and **Fig. 10**. The path loss of zone *II* based on the hybrid model and RSSI observations is shown in **Fig. 11** and **Fig. 12**.

Table 2. Parameters of the hybrid model of path loss through wall based on RSSI observations.

| Transmitting node coordinates (m) | attenuation constant α (Np/m) | relative permittivity ϵ_r | RMSE (dB) |
|-----------------------------------|--------------------------------------|------------------------------------|-----------|
| (-1,0) | 8.9969 | 0.2930 | 6.0803 |
| (-2,0) | 7.6205 | 0.2132 | 6.1968 |

The path loss of zone II corresponding to Tn1(-1, 0) based on statistical model

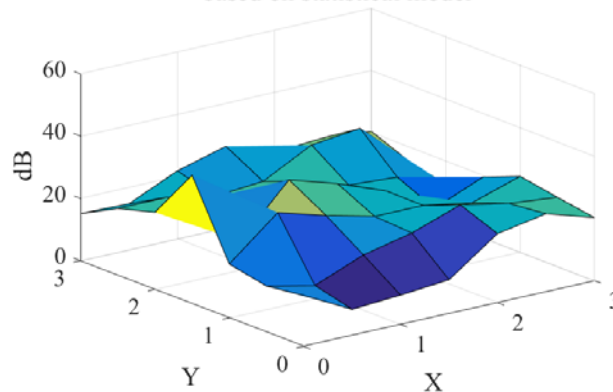


Fig. 9. The path loss of zone *II* corresponding to Tn1(-1,0) based on the statistical model and RSSI observations

The path loss of zone II corresponding to Tn2(-2, 0) based on statistical model

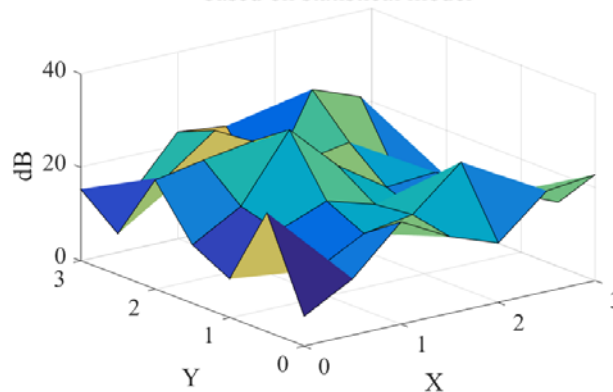


Fig. 10. The path loss of zone *II* corresponding to Tn2(-2,0) based on the statistical model and RSSI observations

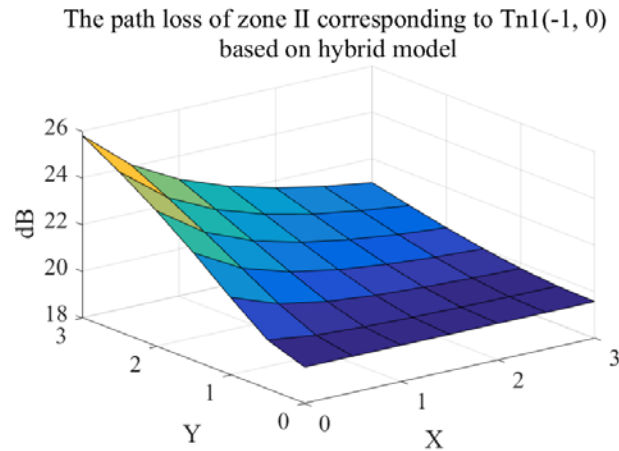


Fig. 11. The path loss of zone II corresponding to Tn1(-1,0) based on the hybrid model and RSSI observations

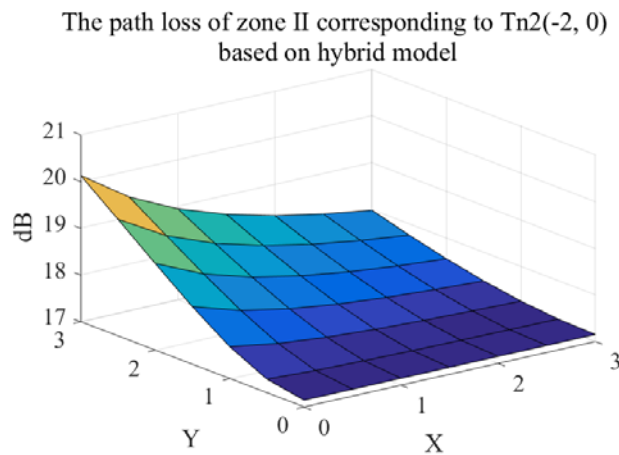


Fig. 12. The path loss of zone II corresponding to Tn2(-2,0) based on the hybrid model and RSSI observations

As can be seen from **Fig. 9** and **Fig. 10**, the established statistical model of path loss through wall shows great fluctuation of path loss corresponding to each grid point due to RSSI observations error, failing to express the actual trend of regional path loss. For the hybrid model of path loss through wall, the denoising RSSI observations and least square method are used to solve the attenuation constant and relative permittivity, and the observation RSSI error of partial receiving nodes can be reduced. As can be seen from **Fig. 11** and **Fig. 12**, the hybrid model can well express the trend and regional continuity of path loss through wall.

For the hybrid model of path loss corresponding to the transmitting node at different positions, the path loss trend is basically the same, and the solved relative permittivity and the attenuation constant have small differences. The path loss difference of the transmitting node Tn1 at position (-1,0) is 2-4dB compared with that of the transmitting node Tn2 at position (-2,0), and the RMSE of the corresponding hybrid model is slightly smaller. The result indicates that the hybrid model is also affected by RSSI observations error, and the regional path loss is independent of the position of the transmitting node.

3.4 The verification of the hybrid model validity

The validity of the hybrid model is analyzed from three aspects: unknown material wall, model accuracy and prediction ability. In the RSSI observation experiment, the wall material is unknown. The path loss is calculated by the theoretical model based on the empirical values of electromagnetic characteristic parameters and the hybrid model based on measured RSSI, respectively. By comparing the relative permittivity and attenuation constants in [Table 1](#) and [Table 2](#), the empirical value of the concrete wall is close to the calculated value of the unknown material wall. Accordingly, from [Fig. 7](#), [Fig. 8](#), [Fig. 11](#) and [Fig. 12](#), the trend of path loss calculated by the theoretical model and the hybrid model is basically the same, and the path loss at the corresponding position has a difference of 3-5dB. The RMSE calculated in the modeling process of hybrid model represents the internal accuracy of the model. From [Table 2](#), the RMSE of the hybrid model established corresponding to Tn1(-1,0) and Tn2(-2,0) is 6.0803 and 6.1968, respectively. The RMSE of the hybrid model is basically consistent with the fluctuation range of the RSSI observations. Therefore, the hybrid model can be used to calculate the path loss of the signals through the wall.

In order to verify the prediction ability, the hybrid model are used to inversely calculate the RSSI of each grid points in zone *III*, which is an extended region. The RSSI observations of receiving nodes in zone *III* are not participate in the establishment of the hybrid model, and are only used for comparison with inversely calculated RSSI. The measured RSSI and inversely calculated RSSI corresponding to Tn1 and Tn2 are shown in [Fig. 13](#) and [Fig. 14](#), respectively.

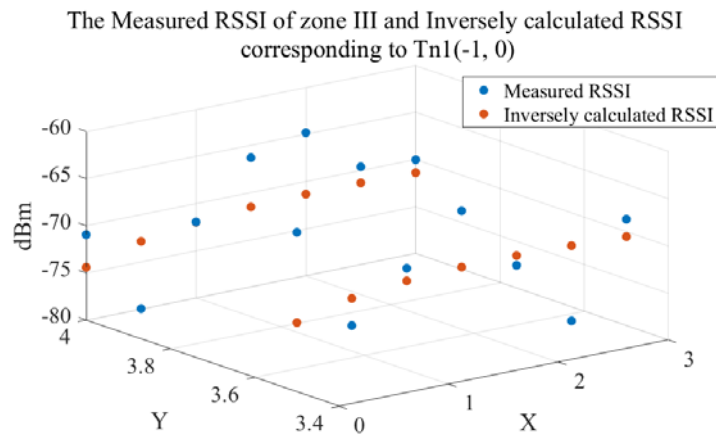


Fig. 13. The measured RSSI of zone *III* and inversely calculated RSSI corresponding to Tn1(-1,0)

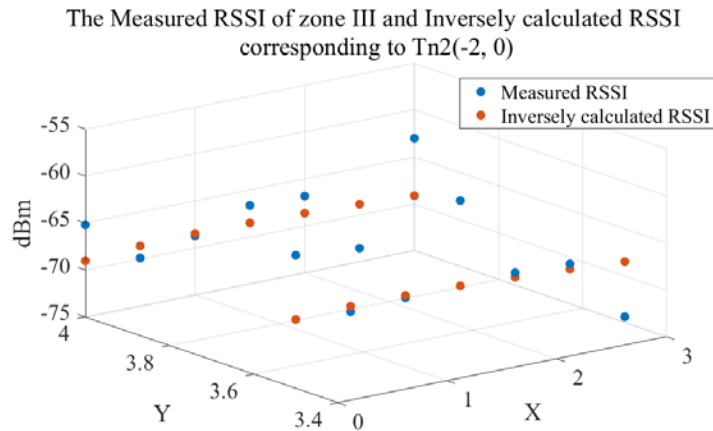


Fig. 14. The measured RSSI of zone III and inversely calculated RSSI corresponding to Tn2(-2,0)

As can be seen from **Fig. 13** and **Fig. 14**, the inversely calculated RSSI by the hybrid model is basically consistent with the measured RSSI. The RMSE of measured RSSI and inversely calculated RSSI corresponding to Tn1 is 4.9520, and the RMSE of measured RSSI and inversely calculated RSSI corresponding to Tn2 is 4.204. The RMSE of measured RSSI and inversely calculated RSSI is the external accuracy of the hybrid model, represents the prediction ability of the model. The results show that the hybrid model can be used to predict the regional path loss. However, the accuracy of hybrid model and the effect of model prediction are affected by RSSI observation errors. In addition, the heterogeneity of wall materials also affects the accuracy of modeling and model prediction.

4. Conclusion

The localization validity of RSSI can be improved by modeling and correcting the path loss of wireless signals through the wall. The theoretical model of path loss of wireless signals through the wall is difficult to obtain the accurate electromagnetic characteristic parameters in practical scenarios, and the path loss solved by the statistical model of wireless signals through wall has irregular fluctuation and discontinuity of adjacent areas. The hybrid model of path loss of signals through the wall is proposed by combining the theoretical model and statistical model. The theoretical model can be established by the empirical values of electromagnetic characteristic parameters of the concrete wall. The path loss increases with the increase of incident angle, and increases sharply with the incident angle from 70° to 89° . The wall thickness has a great influence on the path loss, followed by the attenuation constant, and the relative permittivity has a small influence on the path loss. However, if the wall material is unknown, the electromagnetic characteristics of the wall cannot be obtained, and the theoretical model of the path loss of the wireless signals through the wall cannot be established. Based on the RSSI observation experiment, the statistical model and the hybrid model of path loss of signals through wall are established, respectively. The results show that the hybrid model not only solves the inaccurate empirical values of electromagnetic propagation parameters in the theoretical model, but also weakens the influence of RSSI observation errors in the statistical model. The hybrid model can well express the actual trend of regional path loss and maintain the path loss continuity of adjacent areas, and can be used to predict the regional path loss.

References

- [1] M. Zhou, X. Li, Y. Wang, Y. Li, A. Ren, "Indoor intrusion detection based on deep signal feature fusion and minimized-MKMMMD transfer learning," *Phys. Commun.*, vol.42, pp.1-11, 2020. [Article \(CrossRef Link\)](#)
- [2] Ompal, V. M. Mishra, A. Kumar, "FPGA integrated IEEE 802.15.4 ZigBee wireless sensor nodes performance for industrial plant monitoring and automation," *Nucl. Eng. Technol.*, vol.54, no.7, pp. 2444- 2452, 2022. [Article \(CrossRef Link\)](#)
- [3] E. P. Kho, S. N. D. Chua, S. F. Lim, L. C. Lau, M. T. N. Gani, "Development of young sago palm environmental monitoring system with wireless sensor networks," *Comput Electron Agric.*, vol.193, pp.1-12, 2022. [Article \(CrossRef Link\)](#)
- [4] S. Djosic, I. Stojanovic, M. Jovanovic, G. Lj. Djordjevic, "Multi-algorithm UWB-based localization method for mixed LoS/NLoS environments," *Comput. Commun.*, vol.181, pp.365-373, 2022. [Article \(CrossRef Link\)](#)
- [5] J. Wei, H. Wang, S. Su, Y. Tang, X. Guo, X. Sun, "NLoS identification using parallel deep learning model and time-frequency information in UWB-based positioning system," *Meas.*, vol.195, pp.1-9, 2022. [Article \(CrossRef Link\)](#)
- [6] A. Raheemah, N. Sabri, M.S. Salim, P. Ehkan, R. B. Ahmad, "New empirical path loss model for wireless sensor networks in mango greenhouses," *Comput. Electron. Agric.*, vol.127, pp.553-560, 2016. [Article \(CrossRef Link\)](#)
- [7] A. Booranawong, K. Sengchuai, N. Jindapetch, "Implementation and test of an RSSI-based indoor target localization system: Human movement effects on the accuracy," *Meas.*, vol.133, pp.370-382, 2019. [Article \(CrossRef Link\)](#)
- [8] L. Qiyue, W. Zhong, L. Jie, S. Wei, W. Jianping, "A novel adaptive Kalman filter based NLoS error mitigation algorithm," *IFAC-Papers*, vol.48, no.28, pp.1118-1123, 2015. [Article \(CrossRef Link\)](#)
- [9] H. Zheng, Z. Fan, J. Li, "Simulation of electromagnetic wave propagations in negative index materials by the localized RBF-collocation method," *Eng Anal Bound Elem*, vol.136, pp.204-212, 2022. [Article \(CrossRef Link\)](#)
- [10] S. J. Delfim, R. de M. L. Danielle, "Electromagnetic wave propagation analysis by an explicit adaptive technique based on connected space-time discretizations," *Finite Elem Anal Des*, vol.141, pp.1-16, 2018. [Article \(CrossRef Link\)](#)
- [11] M. Bonazzoli, F. Rapetti, C. Venturini, "Dispersion analysis of triangle-based Whitney element methods for electromagnetic wave propagation," *Appl. Math. Comput.*, vol.319, pp.274-286, 2018. [Article \(CrossRef Link\)](#)
- [12] J.V. Balbastre, L. Nuño, "Modelling the propagation of electromagnetic waves across complex metamaterials in closed structures," *J. Comput. Appl. Math.*, vol.352, pp.40-49, 2019. [Article \(CrossRef Link\)](#)
- [13] S. H. Lessly, R. Senthil, U. Ellampooranan, "Studies on the effect of inclination of reinforcement and wave propagation in concrete cores through finite element simulations," *Mater. Today: Proc.*, vol.45, pp.6533-6541, 2021. [Article \(CrossRef Link\)](#)
- [14] X. Wei, Y. Chang, M. Lin, H. Xu, Y. Li, X. Han, "Study on the influence of thin plasma thickness on electromagnetic wave attenuation," *Vacuum*, vol.191, pp.1-9, 2021. [Article \(CrossRef Link\)](#)
- [15] G. Shi, Y. He, B. Li, L. Zuo, B. Yin, W. Zeng, F. Ali, "Analysis and modeling of wireless channel characteristics for Internet of Things scene based on geometric features," *Future Gener Comput Syst*, vol.101, pp.492-501, 2019. [Article \(CrossRef Link\)](#)
- [16] S. I. Popoola, A. A. Atayero, O. A. Popoola, "Comparative assessment of data obtained using empirical models for path loss predictions in a university campus environment," *Data Br.*, vol.18, pp.380-393, 2018. [Article \(CrossRef Link\)](#)
- [17] S. Phoemphon, C. So-In, N. Leelathakul, "Improved distance estimation with node selection localization and particle swarm optimization for obstacle-aware wireless sensor networks," *Expert Syst. Appl.*, vol.175, pp.1-20, 2021. [Article \(CrossRef Link\)](#)

- [18] Q. Ren, Y. Zhang, I. Nikolaidis, J. Li, Y. Pan, "RSSI quantization and genetic algorithm based localization in wireless sensor networks," *Ad Hoc Networks*, vol.107, pp.1-8, 2020. [Article \(CrossRef Link\)](#)
- [19] D. Park, W. K. Chung, J. Kim, "Analysis of Electromagnetic Waves Attenuation for Underwater Localization in Structured Environments," *Int J Control Autom Syst.*, vol.18, no.3, pp.575-586, 2020. [Article \(CrossRef Link\)](#)
- [20] K. Hao , Y. Gao, J. Du, X. Wang, J. Zhang, S. Yang, Z. Li, "One-dimensional photonic crystal transparent wall with wide-angle and polarization-insensitive for 5G signal transmission," *Optik*, vol.242, pp.1-10, 2021. [Article \(CrossRef Link\)](#)
- [21] G. Shi, Y. He, B. Li, L. Zuo, B. Yin, W. Zeng, F. Ali, "Analysis and modeling of wireless channel characteristics for Internet of Things scene based on geometric features," *Future Gener Comput Syst.*, vol.101, pp.492-501, 2019. [Article \(CrossRef Link\)](#)
- [22] P. Hu, J. Yang, L. Guo, X. YU, W. LI, "Solar-tracking methodology based on refraction-polarization in Snell's window for underwater navigation," *Chinese J. Aeronaut.*, vol.35, no.3, pp.380-389, 2022. [Article \(CrossRef Link\)](#)
- [23] S. Narieda, T. Fujii, K. Umebayashi, "Energy constrained optimization for spreading factor allocation in LoRaWAN," *Sensors*, vol.20, no.16, pp.1-15, 2020. [Article \(CrossRef Link\)](#)
- [24] G. Kaur, S. H. Gupta, H. Kaur, "Optimizing the LoRa network performance for industrial scenario using a machine learning approach," *Comput Electr Eng*, vol.100, pp.1-16, 2022. [Article \(CrossRef Link\)](#)
- [25] Y. Rao, Z. H. Jiang, N. Lazarovitch, "Investigating signal propagation and strength distribution characteristics of wireless sensor networks in date palm orchards," *Comput Electron Agric*, vol.124, pp.107-120, 2016. [Article \(CrossRef Link\)](#)
- [26] I. Kaplanvural, K. Özkap, E. Pekşen, "Influence of water content investigation on GPR wave attenuation for early age concrete in natural air-drying condition," *Construction and Building Materials*, vol. 297, pp.1-9, 2021. [Article \(CrossRef Link\)](#)
- [27] M. Ramaniraka, S. Rakotonarivo, C. Payan, V. Garnier, "Effect of the Interfacial Transition Zone on ultrasonic wave attenuation and velocity in concrete," *Cement and Concrete Research*, vol. 124, pp. 1-7, 2019. [Article \(CrossRef Link\)](#)
- [28] W. C. Stone, "Electromagnetic Signal Attenuation in Construction Materials," NIST, Gaithersburg, MD, USA, Tech. Rep. 1997. [Article \(CrossRef Link\)](#)



Guangyong Xi received the B.S. degree in engineering surveying from Hohai University, in 2001, and M.S. degree and the Ph.D. degree in engineering surveying from Hohai University, in 2004 and 2011, respectively. He is an associate professor in the college of computer and communication engineering at Zhengzhou University of Light Industry. His research focuses on IoT information sensing, processing and precise indoors wireless localization.



Shizhen Lin received the B.S. degree in geographic information system from Zhengzhou University, in 2005. He is an engineer in the Shandong Eastdawn Corporation. His research interests are spatial sensing information acquisition, data processing and analysis.



Dongyao Zou received the B.S. degree in industrial automation from Zhengzhou University, in 1996, and the M.S. degree in microelectronics and solid-state electronics and the Ph.D. degree in circuits and systems from the Beijing University of Posts and Telecommunications, in 2005 and 2008, respectively. Since July 2008, he has been engaged in teaching and research work with the college of computer and communication engineering, Zhengzhou University of Light Industry. His research interests include IoT information sensing, processing and node localization technologies.